Civil Engineering and Applied Solutions

Research Article

journal homepage: ceas.journals.umz.ac.ir

CEAS Civil Engineering and Applied Solutions

Comparative Numerical Assessment of Blast Resistance of Steel, Steel–Concrete Composite, and Fiber Metal Laminate Roofs

Hadi Zakeri Khatir [a], Mohammad Javad Shabani [a], Muhamed Shaaebanlu [b*], Mojtaba Araghizadeh [a]

[a] *Faculty of Passive Defense, Malek Ashtar University of Technology, Tehran, Iran*
[b] *Department of Civil Engineering, Shahid Beheshti University, Tehran, Iran*

ARTICLE INFO

Article history:

Received 28 January 2026

Revised 18 February 2026

Accepted 12 May 2026

Available online 01 January 2027

Keywords:

Blast loading

Roof systems

Steel plate deck

Steel–concrete composite

Fiber metal laminate

CFRP

ABSTRACT

Blast loading poses a serious threat to building roof systems due to their relatively low mass and stiffness compared to vertical structural components. This study presents a comprehensive numerical investigation of the blast response of three different roof systems: steel plate deck (SPD), steel–concrete composite deck (SCD), and fiber metal laminate (FML) composed of two steel sheets with intermediate CFRP layers oriented at 0° and 90°. Finite element models were developed in Abaqus to simulate both near-field and far-field blast scenarios using equivalent TNT charges with various stand-off distances and charge weights. A detailed parametric study was conducted to evaluate the influence of key design parameters, including material thickness, explosive weight, and stand-off distance, on the maximum von Mises stress. The results demonstrate that the stand-off distance is the governing parameter controlling the structural response under blast loading. The steel–concrete composite system exhibited the most stable performance due to the combined effects of increased mass, energy absorption, and composite action, while the steel plate deck showed significant plastic deformation under close-in explosions. The FML system provided excellent performance at moderate and large stand-off distances; however, it was highly sensitive to near-field blasts due to the brittle failure characteristics of CFRP layers. Furthermore, blast design charts based on scaled distance were developed and power-law relationships were proposed to enable rapid estimation of maximum stress for preliminary design purposes. The findings provide practical insights for selecting and designing roof systems with improved blast resistance.

How to cite this article: Zakeri, H., Shabani, M., Shaaebanlu, M., Araghizadeh, M. Comparative Numerical Assessment of Blast Resistance of Steel, Steel–Concrete Composite, and Fiber Metal Laminate Roofs. Civil Engineering and Applied Solutions. 2027; 3(1): 61–77. doi:10.22080/ceas.2026.31139.1075.

1. Introduction

Blast loading represents one of the most severe and unpredictable extreme actions that civil engineering structures may experience during their service life [1]. Accidental explosions in industrial facilities, gas detonations, transportation-related incidents, and intentional attacks have demonstrated the catastrophic consequences that blast-induced damage can impose on buildings and infrastructure. Unlike conventional static or quasi-static loads, blast loads are characterized by extremely high peak pressures, very short duration, and complex wave–structure interaction mechanisms [2]. These characteristics may induce intense stress wave propagation, localized failure, progressive collapse, and significant loss of structural integrity [3].

Among structural components, slab and roof systems are particularly vulnerable to blast loading due to their large exposed surface area and relatively limited thickness compared to vertical load-bearing members. Damage to roof structures not only compromises local structural capacity but may also trigger internal pressurization effects and cascading failure of supporting

* Corresponding author.
E-mail addresses: shabanlou@mail.ir (M. Shaaebanlu).

https://doi.org/10.22080/ceas.2026.31139.1075
ISSN: 3092-7749/

elements. Consequently, enhancing the blast resistance of slab and roof systems has become an important research topic in protective structural engineering [4-6].

Extensive experimental and numerical investigations have been conducted on the blast behavior of reinforced concrete (RC) slabs. Previous studies have examined the influence of reinforcement ratio, slab thickness, concrete strength, boundary conditions, and scaled distance on dynamic response and failure modes. It has been shown that slab response may transition from global flexural deformation to localized punching shear as the stand-off distance decreases. In addition, quantitative performance indices such as support rotation angle, residual deflection, and damage level classifications have been proposed to evaluate blast resistance [7]. In parallel, steel plates and steel structural components have been widely studied under impulsive loading. Numerical and experimental investigations have highlighted the significant role of plate thickness, boundary restraint, and strain-rate effects in controlling deformation and failure patterns. Compared with reinforced concrete slabs, steel plates exhibit different energy absorption mechanisms governed primarily by membrane action and plastic yielding [8, 9].

To combine the advantages of steel and concrete, steel–concrete composite (SC) systems have increasingly attracted attention in protective engineering. Composite action between steel plates and concrete cores can enhance stiffness, increase mass participation, and improve energy dissipation capacity. Previous research has demonstrated that SC composite slabs generally exhibit improved blast resistance compared to conventional RC or steel-only systems, although their failure modes depend strongly on charge weight and stand-off distance [10].

More recently, lightweight advanced materials such as fiber-reinforced polymers (FRP) and fiber metal laminates (FML) have been explored for protective applications [11, 12]. These hybrid systems offer high strength-to-weight ratio, corrosion resistance, and favorable fatigue performance. However, despite growing interest in FRP-strengthened and hybrid composite members, systematic investigations of FML roof systems subjected to external blast loading remain limited. In particular, the interaction between metallic layers and brittle composite plies under high-intensity impulsive loading is not yet fully understood.

Although the existing body of literature provides valuable insights into individual structural systems, several limitations remain. First, most studies focus on a single structural configuration, making direct performance comparison among steel plate decks, steel–concrete composite roofs, and fiber metal laminate systems difficult. Second, the majority of numerical investigations report peak stresses or displacements without establishing generalized design-oriented relationships that can assist engineers in rapid preliminary assessment. Third, the mechanical interpretation of blast response in terms of material yielding, damage initiation, and failure mechanisms, especially for hybrid systems involving CFRP layers, has received comparatively limited attention.

In light of these gaps, this study presents a comprehensive comparative numerical assessment of three roof systems: a steel plate deck (SPD), a steel–concrete composite deck (SCD), and a fiber metal laminate (FML) roof configuration subjected to external blast loading. Explicit dynamic finite element simulations [13] are conducted to evaluate stress demand, deformation characteristics, and damage development under varying stand-off distances. Advanced constitutive models are employed to capture material nonlinearity and damage mechanisms. Furthermore, blast design charts based on the scaled distance concept are developed by correlating peak stress demand with scaled distance through regression-based power-law relationships. These charts provide a practical tool for rapid estimation of blast response without requiring detailed numerical analysis.

By systematically comparing three distinct roof systems under identical blast scenarios, this study aims to (i) quantify their relative blast resistance, (ii) interpret the governing material-level failure mechanisms, and (iii) provide generalized performance relationships that may support preliminary protective design and decision-making. The outcomes of this study aim to provide both scientific insight and engineering guidance for the selection and optimization of roof systems in structures exposed to explosive hazards.

2. Methodology

2.1 Research framework

Three roof systems were investigated in this study: steel plate deck (SPD), steel–concrete composite deck (SCD), and fiber metal laminate (FML). All numerical models were developed with identical supporting frames to ensure a consistent basis for comparison.

The study adopts a comparative numerical framework in which three roof configurations are evaluated under identical boundary and loading conditions to ensure a consistent performance basis.

2.2. Parametric study design

A systematic one-variable-at-a-time parametric framework was adopted to quantify the influence of key design variables on the blast response while avoiding confounding effects. For each roof system, the investigated parameters included:

- SPD: steel plate thickness, explosive charge weight, and stand-off distance.
- SCD: concrete thickness, concrete compressive strength f_c', explosive charge weight, and stand-off distance (with steel thickness and reinforcement parameters varied in selected cases).
- FML: steel sheet thickness, CFRP layer thickness, explosive charge weight, and stand-off distance (with the CFRP layup maintained at 0°/90°).

For each parameter set, all other variables were held constant to isolate the primary trend. This structured approach provides a consistent basis for (i) cross-system performance comparison and (ii) development of generalized blast design relationships based on scaled distance. The selected parameters were chosen based on their direct influence on structural stiffness, mass distribution, and energy absorption capacity under blast loading.

2.3. Performance evaluation criteria

The primary response parameter used for performance comparison was the maximum von Mises stress within the roof panel. The von Mises equivalent stress represents a scalar measure of the combined multiaxial stress state at a material point and is widely accepted as a reliable yielding criterion for ductile materials such as structural steel. By integrating the effects of normal and shear stress components into a single parameter, it provides a rational indicator of the onset of plastic deformation and overall stress demand in structural elements subjected to complex loading conditions.

Under blast loading, structural components experience highly transient and non-uniform stress distributions involving bending, membrane action, and shear interaction. Therefore, the maximum von Mises stress was adopted as a consistent and physically meaningful metric for comparing the structural response and damage potential of the investigated roof systems. This approach enables objective cross-system performance evaluation while maintaining a unified comparison basis across different material configurations.

2.4. Scaled distance formulation

To generalize the blast loading scenarios and enable comparison across different explosive weights and stand-off distances, the concept of scaled distance was adopted. The scaled distance Z is defined as $Z = {}^{R}/_{W^{1/3}}$ where R is the stand-off distance, and W is the equivalent TNT charge weight. This formulation, derived from Hopkinson–Cranz scaling law [14, 15], normalizes blast parameters by accounting for the cube-root relationship between explosive energy and distance. As a result, blast scenarios with different combinations of charge weight and stand-off distance but identical scaled distance produce similar pressure–time characteristics.

The use of scaled distance allows the structural response to be interpreted in a dimensionless and generalized manner, thereby facilitating comparison between different blast cases and supporting the development of broader design-oriented relationships beyond the specific numerical values considered in this study.

The overall sequence of steps followed in the present investigation is summarized in Fig. 1. The study begins with the selection of the investigated roof systems (SPD, SCD, and FML) and the definition of key design and loading parameters. Subsequently, detailed finite element models are developed for each configuration. Blast loading scenarios are then applied; Dynamic explicit analyses are performed to capture the transient structural response. Finally, key response parameters, particularly the maximum von Mises stress, are extracted and used for comparative performance assessment and trend evaluation. This structured framework ensures methodological clarity, reproducibility of the analysis procedure, and consistency in cross-system comparison.

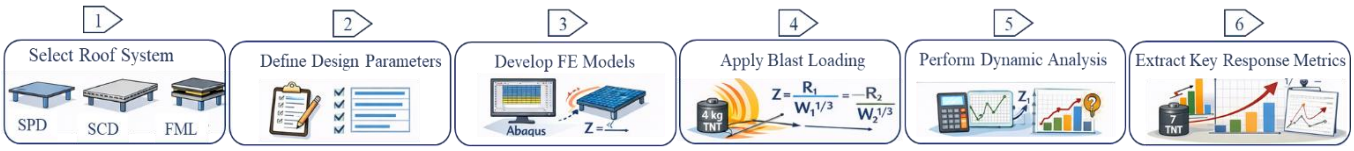

Fig. 1. Schematic flowchart of the research methodology showing the sequential procedure followed in the numerical investigation.

3. Numerical modeling

3.1. Geometry and boundary conditions

The roof panel had a square plan with dimensions of 5 m × 5 m and was connected to the surrounding frame members.

The roof system was modeled as simply supported along its edges, allowing rotation while restraining vertical displacement. This boundary condition was selected to represent typical roof–frame connections in practical structures and to isolate the influence of material configuration and blast parameters on structural response. Beam and column members were modeled using frame elements, while the roof panels (steel plates, concrete slabs, and composite laminates) were modeled using shell elements to accurately capture bending, membrane action, and in-plane stress distribution.

A mesh sensitivity study was conducted to ensure that the numerical results are independent of element size. Several mesh densities were evaluated, and key response parameters including maximum mid-span displacement, peak von Mises stress, and damage initiation indices were monitored. It was observed that refinement beyond an element size of 50 × 50 mm resulted in negligible changes in the primary response quantities, with variations remaining within acceptable numerical tolerance. Given the global dimensions of the slab systems and the focus on comparative structural performance, the 50 × 50 mm mesh was selected as it provides a suitable balance between computational efficiency and solution accuracy. The convergence assessment confirms that the reported results are mesh-independent.

3.2. Material properties and constitutive models

This section thoroughly explains the material properties and constitutive models, including the modeling assumptions.

3.2.1. Steel

Steel components were modeled using elastic–plastic constitutive laws. Two different steel grades were considered to accurately represent the mechanical behavior of structural plates/frames and reinforcing bars in the composite roof system.

For all steel plates and structural frame members (SPD, SCD steel sheets, and FML steel layers), the elastic modulus and Poisson's ratio were taken as E = 206 GPa and ν = 0.30, respectively. Plastic behavior was defined by a yield stress of F_y = 240 MPa and an ultimate tensile stress of F_u = 514 MPa. These properties were used to assess yielding onset, plastic deformation, and potential severe damage in the steel roof components under blast loading. For the reinforcing bars embedded in the concrete layer of the SCD system, a higher-strength steel grade was adopted. The reinforcing steel was modeled with a yield stress of F_y = 400 MPa and an ultimate tensile stress of F_u = 600 MPa, while the elastic modulus and Poisson's ratio were assumed identical to those of structural steel (E = 206 GPa, ν = 0.30). This distinction allows realistic simulation of stress redistribution between the concrete matrix and the steel reinforcement and enables accurate interpretation of reinforcement yielding and post-yield behavior under extreme blast-induced loading.

3.2.2. Concrete

The concrete layer in the steel–concrete composite deck was modeled using the Concrete Damaged Plasticity (CDP) model available in Abaqus to capture nonlinear behavior, cracking in tension, and crushing in compression under dynamic loading [16, 17]. The key CDP parameters adopted in the simulations are tabulated in Table 1.

The concrete compressive strength f_c' and slab thickness were varied as part of the parametric study, while the above CDP parameters were kept constant. This modeling approach enables realistic representation of stiffness degradation and energy dissipation mechanisms that are essential for evaluating blast resistance in composite roof systems.

Table 1. Plastic parameters of concrete in the CDP model.

Dilation Angle	Eccentricity	f_{b0}/f_{c0}	K	Viscosity Parameter
30°	0.1	1.16	0.667	0.001

3.2.3. CFRP layers

In the fiber metal laminate (FML) configuration, carbon fiber reinforced polymer (CFRP) sheets were placed between two steel layers. The CFRP plies were arranged in two orthogonal directions (0°/90°) to enhance in-plane stiffness and improve stress redistribution. CFRP was modeled as an orthotropic elastic material with an elastic modulus of E = 42.7 GPa and Poisson's ratio ν = 0.05. The ultimate tensile strength of CFRP was taken as σ_u = 634 MPa.

To realistically capture progressive damage and failure mechanisms in the composite layers under blast loading, the Hashin damage criterion was employed to predict damage initiation in different failure modes, including fiber tension and compression. Following damage initiation, stiffness degradation was governed by an energy-based damage evolution law, in which the post-failure softening behavior was defined using fracture energy (Table 2 and Table 3). This approach allows gradual stiffness reduction after damage onset and enables accurate simulation of brittle failure and energy dissipation in CFRP layers subjected to high-rate dynamic loading [18, 19].

Table 2. Hashin elastic damage parameters.

E_1 (GPa)	E_2 (GPa)	ν_{12}	G_{12} (GPa)	G_{13} (GPa)	G_{23} (GPa)
42.7	42.7	0.05	4.4	4.4	2.3

Table 3. Hashin elastic damage parameters.

Longitudinal tensile strength (MPa)	Longitudinal compressive strength (MPa)	Transverse tensile strength (MPa)	Transverse compressive strength (MPa)	Longitudinal shear strength (MPa)
643	267	643	267	37

The thickness of each CFRP layer was treated as a parametric variable, while the stacking sequence (0°/90°) and damage model parameters were kept constant in the baseline configuration. This modeling strategy ensures that both elastic response and post-damage softening behavior of the composite layers are appropriately represented in the numerical simulations.

3.3. Blast loading and analysis procedure

Blast loads were applied using the CONWEP (Conventional Weapons Effects Program) formulation implemented in Abaqus [20, 21]. Equivalent TNT charges with different explosive weights W and stand-off distances R were considered to simulate both

far-field and near-field blast scenarios [22, 23]. The pressure–time history generated by the CONWEP model was applied normal to the roof surface, accounting for incident and reflected pressure effects as described in the reference blast model.

Dynamic explicit analyses were performed to capture the highly transient response induced by short-duration, high-intensity blast loading. For each simulation case, the primary response parameter extracted was the maximum von Mises stress in the roof system, which was used as the main metric for evaluating stress demand and comparing the performance of different roof configurations under blast loading. As illustrated in Fig. 2, a 4 kg C4 explosive charge, which is equivalent to 8.22 kg TNT, considering the conversion and safety factors, was placed at 3 m standoff distance.

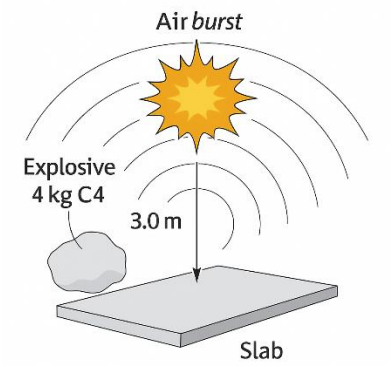

Fig. 2. Schematic view of explosive charge and standoff distance.

3.4. Model validation and verification

The numerical modelling framework adopted in this study is based on previously validated approaches reported in the literature [8, 10, 24, 25]. The Concrete Damage Plasticity (CDP) model has been widely employed in blast and impact simulations of reinforced concrete slabs, demonstrating good agreement with experimental deflection histories, crack patterns, and failure modes. The CDP parameters used herein were selected according to published calibration studies conducted under dynamic loading conditions [16].

Similarly, the Hashin failure criteria and progressive damage modelling for fiber-reinforced laminates have been extensively validated in impact and blast analyses of composite structures. The material properties and failure parameters adopted in the present study are directly taken from experimentally characterized composite systems reported in the literature [11].

The blast loading was defined using the CONWEP formulation, which is based on the empirical Kingery–Bulmash data and has been widely accepted for engineering-level blast simulations [26, 27].

Although a direct specimen-specific experimental validation was not performed for the investigated configurations, the modelling strategy, constitutive parameters, and loading formulation are consistent with previously validated numerical–experimental studies. Moreover, the predicted deformation patterns and failure mechanisms are qualitatively consistent with experimentally reported flexural-dominated behavior in slab-type structures under blast loading.

3.5. Consideration of strain-rate effects

Explosive loading typically generates extremely high strain rates in structural components, commonly in the range of 10^2–10^4 s^{-1}, whereas static loading conditions generally produce strain rates on the order of 10^{-6}–10^{-5} s^{-1} [28-30]. Under such rapid loading, material behavior may deviate significantly from its quasi-static response, potentially altering both strength characteristics and failure modes.

It is well established that increasing strain rate generally enhances the yield strength and ultimate tensile strength of steel. Experimental investigations reported by Chen et al. (2017), McDonald et al. [31], and Norris et al. [32] demonstrate that plastic flow stress increases markedly under impulsive loading conditions. In blast-resistant design practice, this enhancement is commonly accounted for using Strength Increase Factors (SIF) and Dynamic Increase Factors (DIF), whereby static material strengths are amplified to reflect dynamic conditions [23].

Similarly, concrete exhibits rate-dependent enhancement in both compressive and tensile strengths under high strain rates. Although the dynamic modulus of elasticity of steel remains essentially unchanged, concrete may experience a slight increase. These variations influence stiffness and cracking response under blast loads.

In the present study, strain-rate enhancement factors were not explicitly incorporated into the constitutive models of steel, concrete, or CFRP materials. Static material properties were adopted for all simulations. This modelling choice was made to ensure consistent and directly comparable baseline behavior across the roof systems under identical loading scenarios. It is acknowledged that neglecting strain-rate effects may lead to conservative predictions of strength for steel and concrete components under near-field blast conditions, as their actual dynamic strength would be higher than the static values used herein.

For CFRP layers, available literature [33-35] indicates that although some rate sensitivity exists, the magnitude of dynamic enhancement is generally lower than that observed in metals and concrete. Therefore, omission of strain-rate effects is not expected

to alter the relative ranking of the investigated roof systems but may influence the absolute magnitude of reported stresses.

Accordingly, the results presented herein should be interpreted as conservative estimates of structural resistance, particularly for near-field scenarios. Incorporation of fully rate-dependent constitutive models represents an important direction for future work.

4. Results

4.1. Overall numerical trends

The numerical results indicate that the blast response of the roof systems is primarily governed by the stand-off distance, while the explosive charge weight plays a secondary role. For all configurations, decreasing the stand-off distance leads to a highly nonlinear increase in the maximum von Mises stress. Moreover, the overall response is strongly influenced by the structural configuration and energy dissipation mechanisms rather than by material strength alone.

For very small stand-off distances (0.5 m and 0.1 m), all roof systems exhibit severe nonlinear behavior, including extensive plasticity in steel components and progressive damage in composite layers. These findings confirm that system-level characteristics such as mass distribution, stiffness, and composite action are critical in mitigating blast-induced damage.

4.2. Steel plate deck (SPD)

The effects of steel plate thickness, standoff distance, and explosive charge weight on the behavior of the steel plate deck are investigated in the following sections.

4.2.1. Effect of steel plate thickness

Fig. 3 illustrates the effect of steel plate thickness on the maximum von Mises stress for the SPD system at a stand-off distance of 3 m and an explosive weight of 8.22 kg. Increasing the plate thickness leads to a substantial reduction in stress demand. Specifically, reducing the thickness from 20 mm to 3 mm results in an increase in peak stress from approximately 68 MPa to nearly 280 MPa, corresponding to an increase of more than 300%.

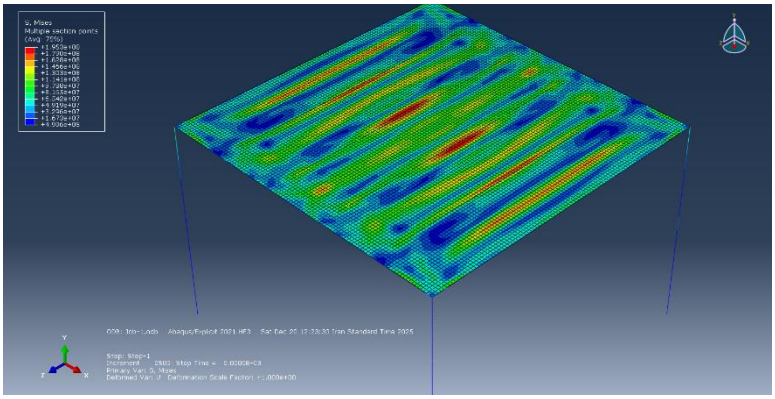

Fig. 3. Von Mises stress of the steel plate deck (SPD) at ultimate state by a stand-off distance of 3 m and an explosive charge of 8.22 kg TNT equivalent.

Thin plates (3–5 mm) clearly exceed the yield stress of structural steel (240 MPa), indicating the onset of widespread plastic deformation. In contrast, thicker plates exhibit significantly lower stress levels, remaining largely within the elastic or near-yield regime (Fig. 4). This behavior is attributed to the increase in flexural stiffness and membrane capacity with thickness.

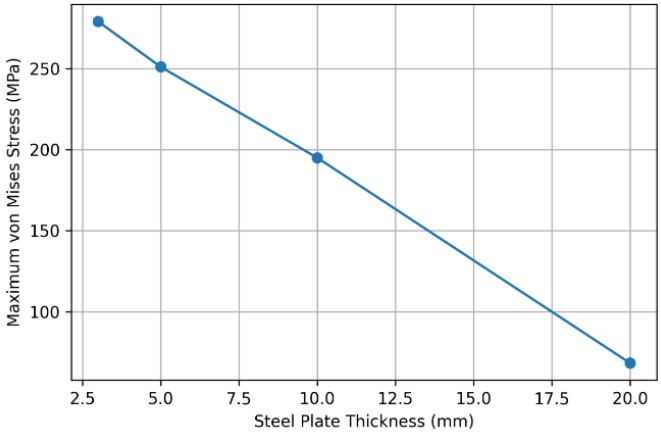

Fig. 4. Effect of steel plate thickness on the maximum von Mises stress of the steel plate deck (SPD) at a stand-off distance of 3 m and an explosive charge of 8.22 kg TNT equivalent.

4.2.2. Effect of stand-off distance

The sensitivity of the SPD system to stand-off distance is shown in Fig. 5, where the maximum stress is normalized by the steel yield stress. At distances of 4–5 m, the normalized stress remains well below unity, indicating elastic behavior. However, when the distance decreases below 2 m, the stress rapidly exceeds the yield limit. At 0.1 m, the normalized stress reaches nearly 2.0, corresponding to a von Mises stress of approximately 470 MPa.

These results demonstrate that the SPD system is extremely vulnerable to near-field explosions, with stress levels approaching the ultimate tensile strength of steel (514 MPa), suggesting a high risk of rupture and severe permanent deformation.

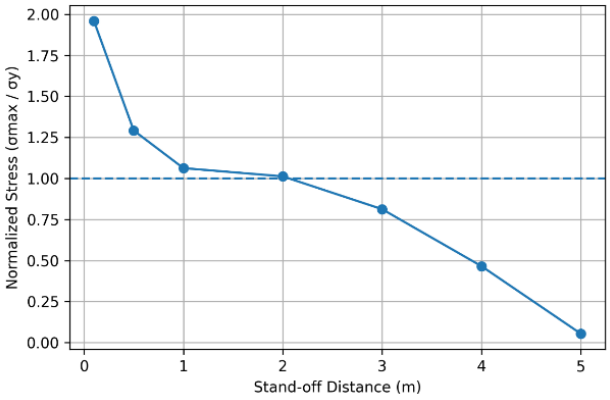

Fig. 5. Normalized maximum von Mises stress (σ_{max}/σ_y) versus stand-off distance for the SPD system with a steel plate thickness of 10 mm under an 8.22 kg TNT equivalent blast.

4.2.3. Effect of explosive charge weight

Fig. 6 presents the influence of TNT equivalent weight at a fixed stand-off distance of 3 m and plate thickness of 10 mm. Increasing the charge weight from 4.11 kg to 24.66 kg increases the maximum stress from approximately 117 MPa to 247 MPa. Although the effect of charge weight is evident, it is less pronounced than that of stand-off distance, confirming that proximity to the blast source is the dominant parameter.

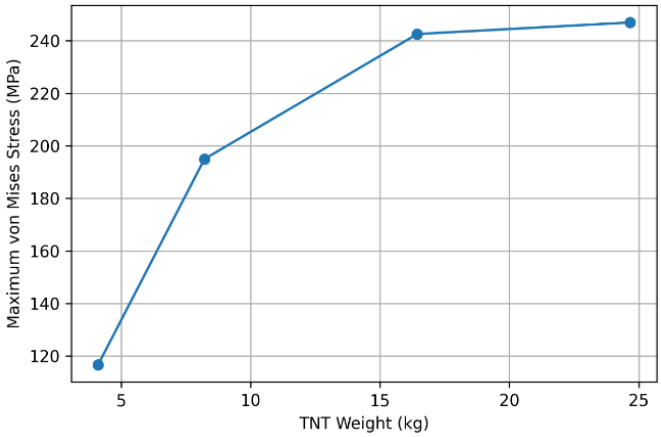

Fig. 6. Influence of TNT equivalent charge weight on the maximum von Mises stress of the SPD system at a stand-off distance of 3 m and a steel plate thickness of 10 mm.

4.3. Steel–concrete composite deck (SCD)

The effects of concrete thickness, concrete compressive strength, standoff distance, and explosive charge weight in the behavior of the steel plate deck are investigated in the following sections.

4.3.1. Concrete damage evaluation using DAMAGET

To further evaluate the capability of the adopted constitutive model in capturing tensile damage under blast loading, the tensile damage variable (DAMAGET) obtained from the Concrete Damage Plasticity (CDP) model is presented. DAMAGET ranges from 0 (undamaged material) to 1 (fully cracked tensile failure), allowing a clear visualization of crack initiation and propagation within the slab.

For the near-field blast scenario, as shown in Fig. 7, the contour distribution of DAMAGET indicates that the tensile damage parameter approaches a value close to 1.00 over a large portion of the slab surface. The highest damage concentration is observed at the mid-span region, where flexural demand and reflected blast pressure are maximum. The widespread distribution of serious damage indices confirms the severe tensile cracking induced by the impulsive loading.

The results demonstrate that the adopted CDP formulation effectively captures the spatial extent and intensity of tensile cracking.

The near-unity damage values across the slab are consistent with the expected flexural failure mechanism under near-field blast conditions, indicating that the model realistically reproduces the progressive degradation of concrete stiffness and strength.

While material-specific damage parameters were used to characterize local failure mechanisms, a unified comparison among all investigated specimens was performed using the von Mises stress distribution. Although von Mises stress does not directly represent a failure criterion for brittle materials, it reflects the intensity of the multiaxial stress state and serves as a consistent indicator of global structural demand under blast loading. This approach enables a rational comparison of overall performance across different structural systems subjected to identical loading conditions.

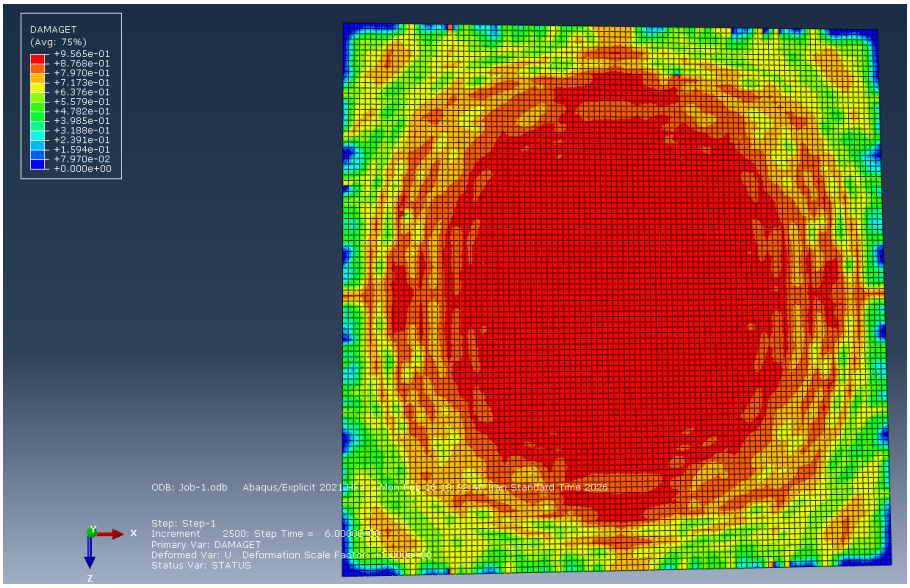

Fig. 7. Contour distribution of tensile damage variable (DAMAGET) for the steel–concrete composite slab under near-field blast loading.

4.3.2. Effect of concrete thickness

Increasing the concrete thickness from 50 mm to 200 mm leads to a marked reduction in the maximum von Mises stress, from approximately 96 MPa to about 43 MPa (Fig. 8). The influence of concrete slab thickness on the blast response is illustrated in Fig. 9. This demonstrates that increasing the effective mass and flexural stiffness of the composite section significantly improves blast resistance.

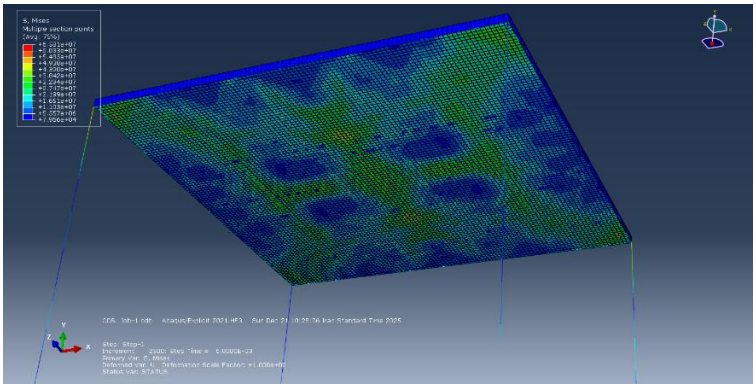

Fig. 8. Von Mises stress of the steel–concrete composite deck (SCD) at a stand-off distance of 3 m under an 8.22 kg TNT equivalent blast.

4.3.3. Effect of concrete compressive strength

Fig. 10 shows the effect of concrete compressive strength f_c' under identical geometric and loading conditions. Variations in f_c' from 15 MPa to 35 MPa result in only minor changes in stress levels. This indicates that, unlike thickness, material strength has a limited influence on the global blast response, which is primarily governed by inertia and stiffness rather than compressive capacity.

4.3.4. Effect of stand-off distance

The variation of maximum stress with stand-off distance for the baseline SCD configuration is shown in Fig. 11. At distances greater than 3–5 m, the stress remains below 25 MPa, indicating a predominantly elastic response. As the stand-off distance decreases below 1 m, the stress increases sharply, exceeding 240 MPa and reaching approximately 242 MPa at 0.1 m.

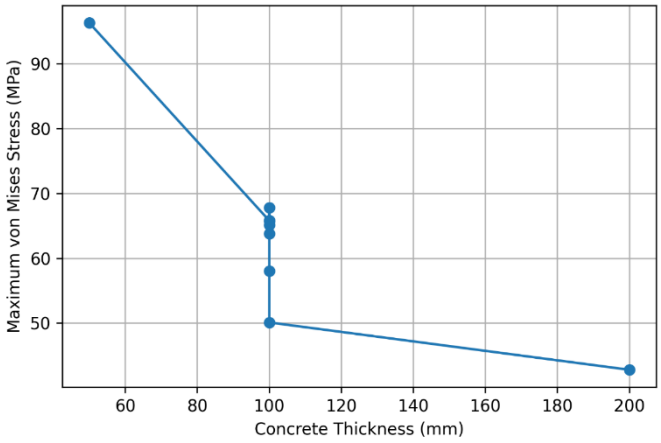

Fig. 9. Effect of concrete slab thickness on the maximum von Mises stress of the steel–concrete composite deck (SCD) at a stand-off distance of 3 m under an 8.22 kg TNT equivalent blast.

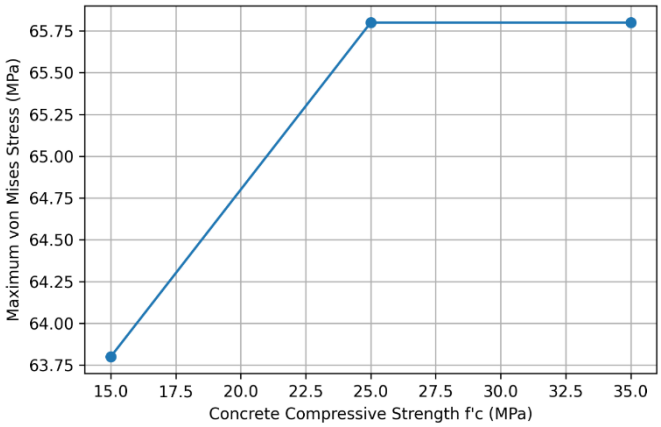

Fig. 10. Effect of concrete compressive strength f’c on the maximum von Mises stress of the SCD system for identical geometric and loading conditions (R = 3 m, W = 8.22 kg).

Although these stress levels indicate yielding of the structural steel components, the reinforcing bars, modeled with a higher yield stress of 400 MPa, remain largely elastic until more severe loading is applied. This promotes stress redistribution and delays localized failure.

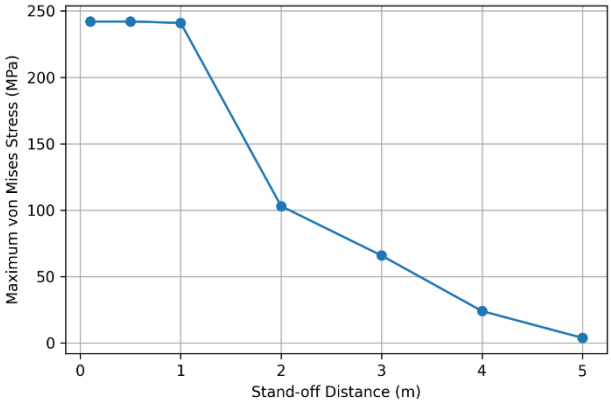

Fig. 11. Variation of maximum von Mises stress with stand-off distance for the baseline SCD configuration (3 mm steel plate + 100 mm concrete slab, fc′=25 MPa, reinforcement diameter = 12 mm) under an 8.22 kg TNT blast.

4.4. Fiber metal laminate (FML)

4.4.1. Failure criterion assessment using HSNFTCRT

To complement the damage evaluation, the Hashin fiber tensile failure criterion (HSNFTCRT) is examined for the composite slab configuration. The HSNFTCRT parameter represents the fiber tensile damage index, where values approaching 1.0 indicate initiation of fiber rupture.

For the near-field blast case, as can be seen in Fig. 12, the HSNFTCRT contour plot shows that the damage index reaches values close to 1.0 at the central region of the slab. This region corresponds to the maximum bending moment and tensile stresses generated by the high-intensity impulsive load. The localization of near-unity values at mid-span confirms the critical role of flexural tensile

stresses in governing the failure response.

The concentration of HSNFTCRT values near 1.0 under severe loading demonstrates that the implemented composite material model successfully captures fiber-dominated tensile failure. The predicted failure pattern aligns with the expected structural behavior of fiber-reinforced systems subjected to high-rate dynamic loading.

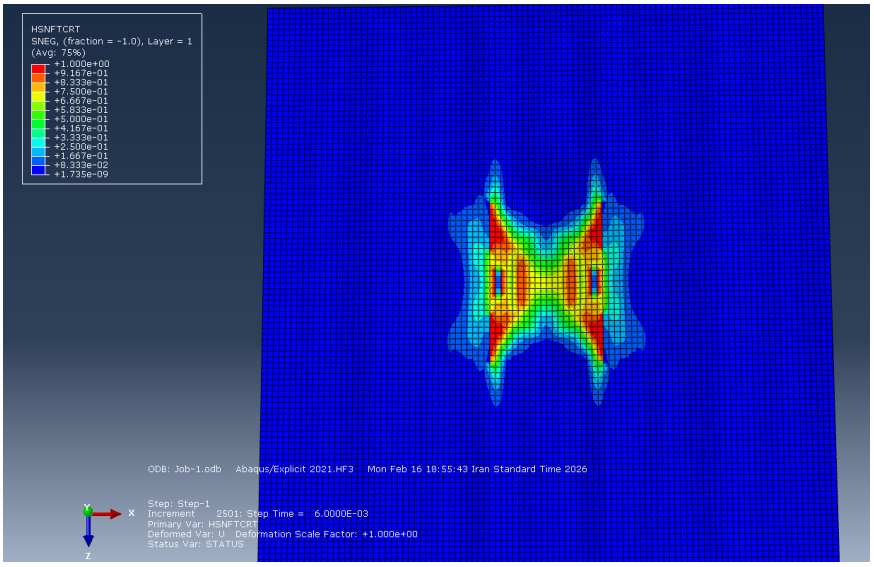

Fig. 12. Contour distribution of Hashin fiber tensile failure index (HSNFTCRT) for the composite laminate system under near-field blast loading.

4.4.2. Effect of steel layer thickness

Fig. 13 illustrates the influence of steel layer thickness on the FML system at a stand-off distance of 3 m. Increasing the steel thickness from 1 mm to 10 mm reduces the maximum stress from approximately 250 MPa to about 55 MPa, demonstrating that the metallic layers play the dominant role in resisting blast-induced bending and membrane forces (Fig. 14).

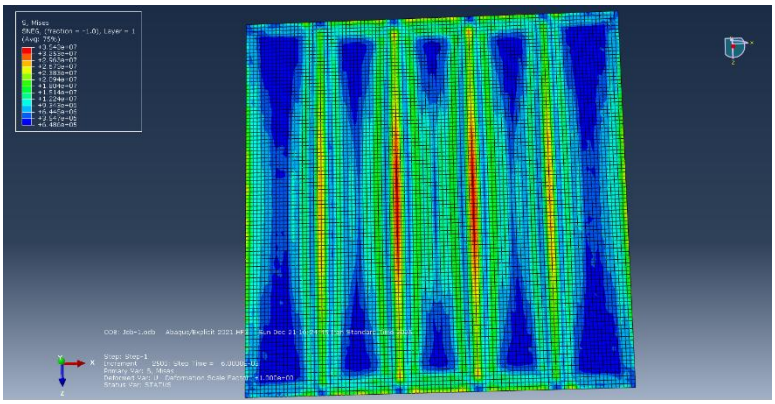

Fig. 13. Von Mises stress of the fiber metal laminate (FML) roof system at a stand-off distance of 3 m and an explosive charge of 8.22 kg TNT equivalent.

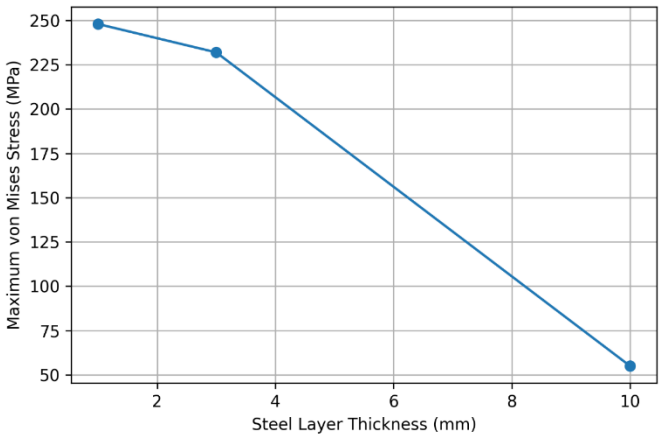

Fig. 14. Effect of steel layer thickness on the maximum von Mises stress of the fiber metal laminate (FML) roof system at a stand-off distance of 3 m and an explosive charge of 8.22 kg TNT equivalent.

4.4.3. Effect of CFRP layer thickness

The effect of CFRP layer thickness is shown in Fig. 15. Increasing the thickness from 0.5 mm to 2 mm results in a moderate reduction in stress. Although CFRP contributes to in-plane stiffness and stress redistribution, its influence is clearly secondary compared to that of the steel layers.

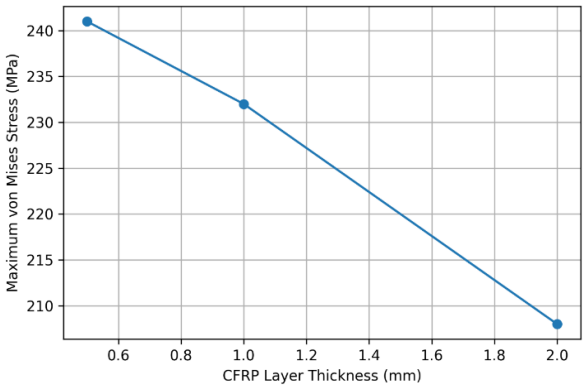

Fig. 15. Effect of CFRP layer thickness on the maximum von Mises stress of the FML system at a stand-off distance of 3 m with a steel layer thickness of 3 mm and an 8.22 kg TNT equivalent blast.

4.4.4. Effect of stand-off distance

Fig. 16 presents the variation of maximum stress with stand-off distance for the baseline FML configuration. At a distance of 5 m, the stress drops to approximately 5 MPa, indicating excellent far-field performance. However, as the distance decreases, the stress rises sharply, reaching about 439 MPa at 0.5 m and approximately 625 MPa at 0.1 m.

These values approach or exceed the ultimate tensile strength of CFRP (634 MPa), indicating the initiation of fiber tensile failure, matrix cracking, and progressive stiffness degradation according to the Hashin damage criterion with energy-based evolution.

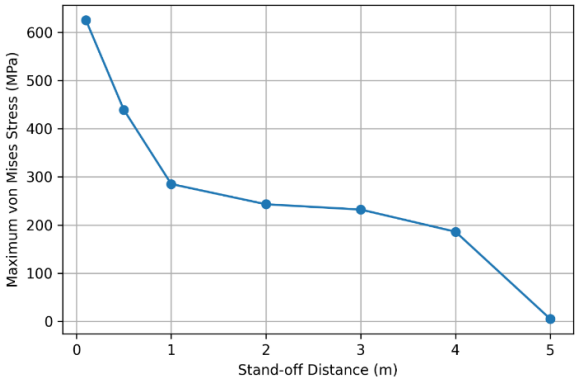

Fig. 16. Variation of maximum von Mises stress with stand-off distance for the baseline FML configuration (3 mm steel + 2 × 1 mm CFRP layers) under an 8.22 kg TNT equivalent blast.

4.5. Comparative performance of roof systems

Fig. 17 compares the three roof systems under identical loading conditions. The SCD system consistently exhibits the lowest stress levels across the entire range of stand-off distances. The SPD system shows rapid stress escalation as the distance decreases, while the FML system, despite its excellent far-field behavior, experiences the highest peak stresses in near-field conditions. This comparison highlights the beneficial role of concrete in increasing effective mass, reducing structural acceleration, and enhancing energy dissipation through cracking, plasticity, and composite interaction.

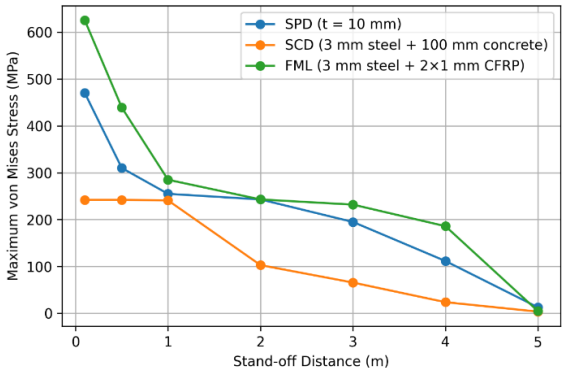

Fig. 17. Comparison of maximum von Mises stress versus stand-off distance for SPD, SCD, and FML roof systems under identical blast loading conditions (W = 8.22 kg TNT equivalent).

4.6. Scaled distance and blast design charts

To assess the universality of the power-law relationship $\sigma_{max} = aZ^{-b}$, two additional simulations with identical scaled distance Z = 1 m/kg^1/3 were performed: (i) R = 2 m, W = 8 kg, and (ii) R = 4 m, W = 64 kg. The von Mises stress contours in Fig. 18 demonstrate that while the overall shape of stress distribution and damage patterns is similar, the far-field scenario with the larger explosive weight exhibits higher peak stresses. To generalize the results, the scaled distance was defined as $Z = R/W^{1/3}$. Fig. 19 shows the variation of maximum von Mises stress with scaled distance for the three systems. As Z decreases, stress increases in a strongly nonlinear manner, particularly in the near-field regime. The SCD system maintains the lowest stress levels over the entire range of Z, while the SPD and FML systems exhibit steeper increases at small Z.

Based on regression analysis, power-law relationships of the form $\sigma_{max} = aZ^{-b}$, were obtained for each system, as illustrated in Fig. 20. These fitted curves provide practical blast design charts that allow rapid estimation of stress levels for different combinations of charge weight and stand-off distance.

Although Hopkinson–Cranz scaling ensures similarity in general blast wave characteristics, the nonlinear structural response is additionally influenced by dynamic interaction effects and strain-rate sensitivity. These results confirm that scaled distance captures general trends in structural behavior, but absolute stress magnitudes depend on the actual explosive charge. Therefore, the derived design charts represent empirical correlations within the investigated parameter domain and are most accurately applied for the specific TNT weight considered, rather than being universally unique scaling laws.

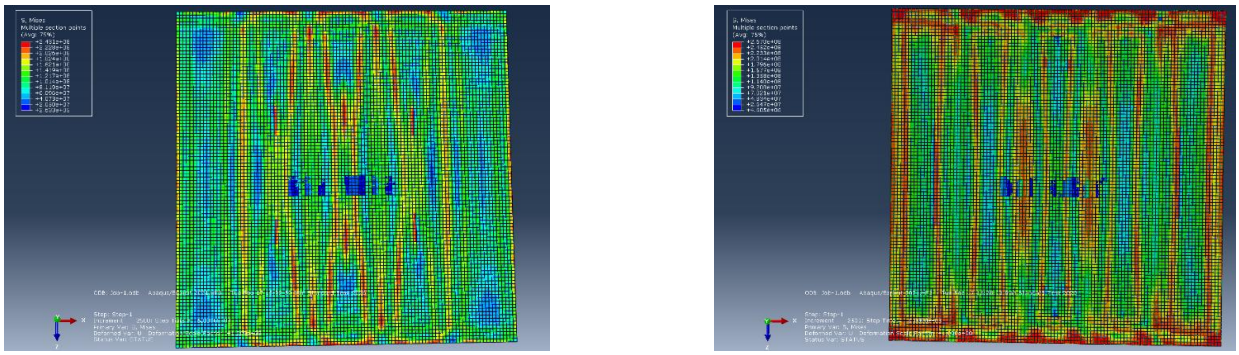

(a) (b)

Fig. 18. Comparison of the predicted ultimate compressive strength from the proposed model based on 1376 experimental circular FRP-confined concrete column specimens.

The SCD system exhibits the lowest baseline stress levels, while the FML system shows the steepest increase in stress at small Z, confirming its vulnerability to near-field explosions.

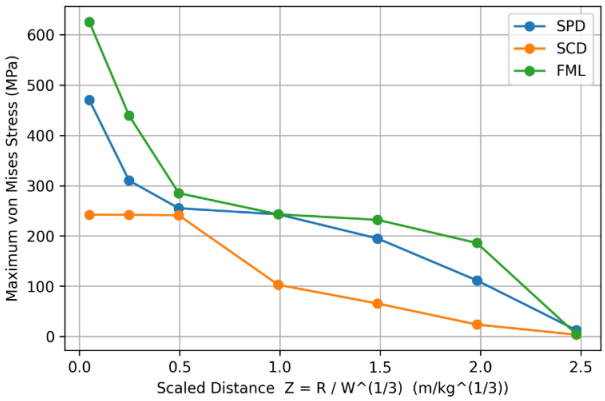

Fig. 19. Maximum von Mises stress as a function of scaled distance Z for SPD, SCD, and FML roof systems based on baseline configurations and an 8.22 kg TNT equivalent blast.

To provide a single, quantitative measure for comparing the blast performance of different roof systems, an integrated performance index was introduced based on the area under the curve (AUC) of maximum von Mises stress versus scaled distance (Z). For each roof system, the von Mises stress at multiple scaled distances was plotted, and the AUC was calculated using numerical integration. This parameter represents the cumulative stress exposure of a system across the range of blast scenarios considered.

In this formulation, lower values of the AUC indicate better blast performance, as the structure experiences lower stress levels over the range of scaled distances, reflecting enhanced resistance to impulsive loading. Conversely, higher AUC values indicate higher cumulative stress and greater vulnerability. Using this approach, as can be seen in Fig. 21, the three investigated systems exhibit the following relative performance: the steel–concrete composite deck (SCD) has the lowest AUC, demonstrating the best overall performance; the steel plate deck (SPD) shows intermediate performance; and the fiber metal laminate (FML) exhibits the highest AUC, indicating the highest susceptibility to near-field and far-field blast effects.

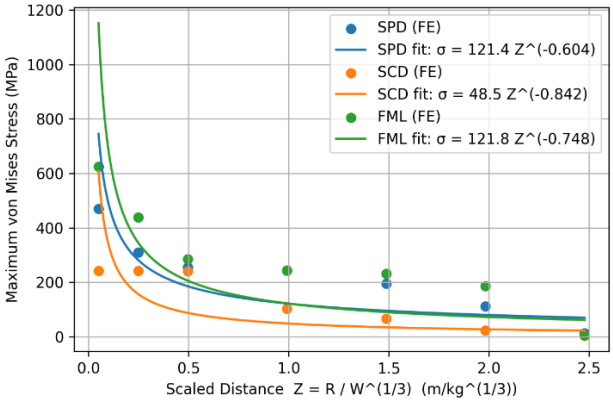

Fig. 20. Blast design chart showing the relationship between maximum von Mises stress and scaled distance for SPD, SCD, and FML roof systems, including power-law fitted curves derived from finite element results.

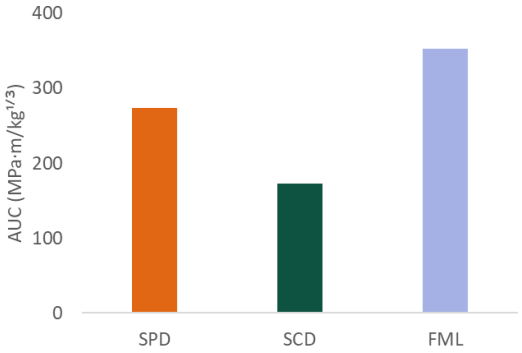

Fig. 21. Integrated performance index (area under σ_{max} –Z curve) for the three roof systems (SPD, SCD, FML). Lower values indicate better blast resistance.

This metric provides a rational and comparative engineering tool, enabling a clear visual and numerical assessment of structural performance under varying blast scenarios, which complements traditional peak stress or damage-based evaluations.

5. Discussion

5.1. Governing parameters in blast response

The numerical results indicate that the stand-off distance is the most critical parameter controlling blast response, while the explosive charge weight plays a secondary role. As the stand-off distance decreases, all roof systems exhibit a highly nonlinear increase in von Mises stress, particularly in near-field conditions. This is consistent with classical blast mechanics, where the incident pressure scales inversely with distance and dominates structural demand.

The structural configuration and energy dissipation mechanisms strongly influence the response. For the SPD system, the blast energy is resisted mainly by plate bending and in-plane tension due to the absence of additional damping mechanisms. In contrast, SCD and FML systems benefit from distributed energy absorption mechanisms (composite action and CFRP layers, respectively), which moderate stress escalation. Therefore, the system-level characteristics, mass distribution, stiffness, and energy dissipation pathways govern performance more than material strength alone.

It should be noted that the CONWEP approach is based on empirical Kingery–Bulmash blast functions developed for spherical or hemispherical TNT charges in air and does not explicitly model detonation-product expansion or gas–structure interaction. In very close-in detonations, particularly within or near the fireball region, the pressure field may be highly non-uniform and influenced by explosive geometry and confinement effects. Nevertheless, CONWEP remains widely used for engineering-level blast analysis due to its computational efficiency and reasonable prediction of free-field and reflected pressures. In this study, since all structural configurations were subjected to identical loading assumptions, the comparative evaluation among specimens remains consistent. However, the absolute magnitudes of stress concentration and localized damage predicted for the smallest stand-off distances should be interpreted considering the inherent limitations of the CONWEP formulation.

5.2. Role of material properties and structural stiffness

For the steel plate deck (SPD), thin plates with thicknesses of 3–5 mm exceed the yield stress of structural steel even under moderate blast loads, while thicker plates tend to remain largely within the elastic range. The increase in plate thickness improves flexural stiffness and activates membrane action, which delays the onset of plastic deformation. However, even substantial increases in thickness do not provide effective resistance against near-field blasts because the SPD system lacks additional energy dissipation mechanisms. As a result, large plastic deformations and potential rupture occur, making the SPD roof the weakest system under close-in explosive scenarios despite its structural simplicity.

The steel–concrete composite deck (SCD) exhibits a more gradual and controlled stress development compared to SPD. Increasing the concrete slab thickness significantly reduces the peak von Mises stress, while variations in compressive strength have only a minor effect on the global response. The concrete layer absorbs blast energy through progressive cracking and crushing, and the reinforcing bars provide post-cracking load-carrying capacity. The composite action between steel, concrete, and reinforcement ensures that stresses are distributed across multiple components, mitigating localized failure. This behavior results in predictable and progressive damage under extreme loads, emphasizing that composite action and overall system mass are more influential for blast mitigation than material strength alone.

In the fiber metal laminate (FML) system, the metallic layers dominate the initial resistance to blast-induced bending and membrane forces, while the CFRP layers contribute to in-plane stress redistribution. Under far-field blast conditions, the FML system exhibits high stiffness and low stress levels, demonstrating excellent performance. However, in near-field scenarios, damage initiation in the CFRP layers leads to rapid stiffness degradation, resulting in a relatively brittle response. Although the FML system offers superior strength-to-weight efficiency and excels in far-field applications, its sensitivity to near-field blasts requires careful design of the CFRP stacking sequence and thickness to prevent abrupt failure.

5.3. Comparative performance of roof systems

The comparative analysis of the three roof systems reveals important design insights. The steel plate deck (SPD) exhibits rapid stress escalation under near-field blasts, leading to large plastic deformations and limited energy dissipation. In contrast, the steel–concrete composite deck (SCD) demonstrates a gradual and predictable response, effectively dissipating energy through concrete cracking and reinforcement action, which results in the most stable overall behavior among the investigated systems. The fiber metal laminate (FML) roof performs exceptionally well under far-field conditions, maintaining low stress levels, but exhibits a relatively brittle response under near-field loading due to the initiation of damage in the CFRP layers.

5.4. Near-field vs far-field behavior

The observations highlight the trade-off between strength, stiffness, and energy absorption. In particular, the distribution of mass and the presence of composite mechanisms often have a more significant impact on blast resistance than simply increasing the material strength. In near-field scenarios, where the scaled distance is small, the SPD and FML systems reach stresses that approach or exceed the yield or ultimate limits, with abrupt failure observed in the FML system once the CFRP layers start to degrade. Conversely, in far-field scenarios with larger scaled distances, all systems remain predominantly elastic, with the FML roof showing the lowest stress levels and demonstrating high efficiency in low-demand conditions. These findings suggest that near-field blast protection favors composite solutions like the SCD, whereas far-field lightweight solutions may benefit from high-strength, efficient systems such as the FML.

5.5. Engineering implications and design recommendations

The results of this study provide several important implications for the blast-resistant design of roof systems in critical and protective structures. Beyond comparing the structural performance of different configurations, the numerical findings offer practical guidance for preliminary design and system selection.

First, the dominant role of stand-off distance highlights the importance of architectural and site-planning strategies in blast mitigation. Increasing the separation between potential explosive sources and structural components is significantly more effective than increasing material strength alone. Even lightweight systems such as FML can perform satisfactorily when adequate stand-off distance is available, whereas all systems become highly vulnerable under near-field conditions.

Second, increasing effective mass and flexural stiffness is shown to be the most efficient structural strategy for improving blast resistance. The steel–concrete composite deck benefits from the inertia of the concrete layer and the composite interaction between steel, concrete, and reinforcement, resulting in reduced acceleration, more uniform stress distribution, and progressive, non-brittle damage mechanisms. From a design perspective, increasing concrete slab thickness is more beneficial than increasing concrete compressive strength, which has only a minor effect on global response.

Third, for lightweight protective systems such as fiber metal laminates, steel layer thickness plays a more critical role than CFRP thickness in controlling peak stress. While CFRP layers enhance in-plane stiffness and strength-to-weight efficiency, near-field blast loading can induce stress levels close to the ultimate tensile capacity of the fibers, leading to rapid damage accumulation and stiffness degradation. Therefore, FML systems should be employed only in applications where blast proximity can be controlled or where weight reduction is the primary design constraint.

Finally, the scaled-distance-based design charts developed in this study provide a practical tool for preliminary assessment of roof performance under explosive loading. The power-law relationships between maximum stress and scaled distance enable rapid estimation of expected stress levels for different charge weights and stand-off distances without the need for time-consuming finite element analyses. These charts can assist engineers in selecting appropriate roof systems, identifying critical loading scenarios, and optimizing geometric parameters in the early stages of blast-resistant design.

6. Conclusions

This study presented a comprehensive numerical investigation of the blast response of three roof systems: steel plate deck (SPD),

steel–concrete composite deck (SCD), and fiber metal laminate (FML). Finite element simulations incorporating realistic material models, including elastic–plastic steel behavior, concrete damaged plasticity, and progressive composite damage using the Hashin criterion with energy-based softening, were used to evaluate structural performance under various blast scenarios. Based on the results, the following conclusions can be drawn:

- Stand-off distance is the governing parameter.
- For all roof systems, the maximum von Mises stress increased in a highly nonlinear manner as the stand-off distance decreased. The influence of explosive charge weight was noticeable but consistently secondary compared to the effect of distance, particularly in near-field blast conditions.
- The steel–concrete composite deck (SCD) exhibited the most stable and reliable performance.
- The presence of the concrete layer significantly increased the effective mass and flexural stiffness of the system, leading to reduced structural acceleration and enhanced energy dissipation through cracking, plasticity, and composite action. Even under severe loading, damage developed gradually, and the reinforcement, modeled with a higher yield stress, contributed to stress redistribution and delayed failure.
- The steel plate deck (SPD) showed the weakest blast resistance in near-field conditions. Although increasing plate thickness reduced stress levels, thin plates rapidly exceeded the steel yield stress and developed extensive plastic deformation. The lack of secondary energy dissipation mechanisms makes this system highly vulnerable to close-in explosions, limiting its suitability for blast-resistant design.
- The fiber metal laminate (FML) system demonstrated excellent far-field efficiency but poor near-field robustness. At moderate and large stand-off distances, FML provided very low stress levels and high strength-to-weight efficiency. However, under near-field loading, stresses approached or exceeded the ultimate tensile strength of CFRP, triggering progressive damage, stiffness degradation, and a relatively brittle global response. Increasing steel layer thickness proved more effective than increasing CFRP thickness in improving blast resistance.
- Increasing effective mass and stiffness is more effective than increasing material strength alone.
- Geometric parameters such as concrete thickness and steel layer thickness had a far greater impact on blast performance than material strength parameters such as concrete compressive strength. This highlights the dominant role of inertia and structural configuration in blast-resistant design.
- The use of the scaled distance parameter enabled generalization of the numerical results for different charge weights and stand-off distances. The derived power-law relationships between maximum stress and scaled distance allow rapid preliminary assessment of roof performance without the need for detailed finite element analyses.
- Overall, the steel–concrete composite roof system is recommended for applications where blast resistance and structural robustness are critical. The fiber metal laminate system is suitable for lightweight structures where sufficient stand-off distance can be ensured, while the steel plate deck is not recommended for near-field blast scenarios.

Statements & Declarations

Author contributions

Hadi Zakeri Khatir: Investigation, Visualization, Validation, Formal analysis, Resources, Writing - Original Draft, Writing - Review & Editing.

Mohammad Javad Shabani: Investigation, Visualization, Validation, Formal analysis, Resources, Writing - Original Draft, Writing - Review & Editing.

Muhamed Shaaebanlu: Conceptualization, Methodology, Formal analysis, Project administration, Supervision, Writing - Review & Editing.

Mojtaba Araghizadeh: Investigation, Resources, Visualization, Writing - Review & Editing.

Funding

The authors received no financial support for the research, authorship, and/or publication of this article.

Data availability

The data presented in this study will be available on request from the corresponding author.

Declarations

The authors declare no conflict of interest.

References

[1] Federal Emergency Management Agency (FEMA). FEMA 427: Risk Management Series: Primer for Design Professionals – Communicating with Owners and Managers of New Buildings on Earthquake Risk. Washington (D.C): FEMA; 2003.

[2] Engineers, U. S. Structures to Resist the Effects of Accidental Explosions. Washington (D.C): U.S. Army Corps of Engineers; 2008. Report No.: UFC 3-340-02.

[3] Luccioni, B. M., Ambrosini, R. D., Danesi, R. F. Analysis of building collapse under blast loads. Engineering Structures, 2004; 26: 63–71. doi:10.1016/j.engstruct.2003.08.011.

[4] Zhao, C., He, K., Zhi, L., Lu, X., Pan, R., Gautam, A., Wang, J., Li, X. Blast behavior of steel-concrete-steel sandwich panel: Experiment and numerical simulation. Engineering Structures, 2021; 246: 112998. doi:10.1016/j.engstruct.2021.112998.

[5] Yao, S., Zhang, D., Chen, X., Lu, F., Wang, W. Experimental and numerical study on the dynamic response of RC slabs under blast loading. Engineering Failure Analysis, 2016; 66: 120–129. doi:10.1016/j.engfailanal.2016.04.027.

[6] Zolghadr Jahromi, H., Izzuddin, B. A., Nethercot, D. A., Donahue, S., Hadjioannou, M., Williamson, E. B., Engelhardt, M., Stevens, D., Marchand, K., Waggoner, M. Robustness Assessment of Building Structures under Explosion. Buildings, 2012; 2: 497–518. doi:10.3390/buildings2040497.

[7] Chen, G. Q., Wu, H., Cheng, Y. H., Lu, J. X. Comparative studies on blast resistance of precast concrete composite and cast-in-place slabs. Journal of Building Engineering, 2025; 110: 113077. doi:10.1016/j.jobe.2025.113077.

[8] Tian, S., Yan, Q., Du, X., Chen, F., Zhang, B. Experimental and numerical studies on the dynamic response of precast concrete slabs under blast load. Journal of Building Engineering, 2023; 70: 106425. doi:10.1016/j.jobe.2023.106425.

[9] Lin, Y., Wang, Y., Wan, S., Yang, C., Zong, Z., Qian, H., Xu, X., Elchalakani, M., Cai, J. Experimental studies on behavior of one-part geopolymer composite slabs subjected to blast loading. Structures, 2024; 66: 106825. doi:10.1016/j.istruc.2024.106825.

[10] Zhu, W., Xiao, Y., Yu, J., Jia, J., Li, Z. Damage modes and mechanism of steel-concrete composite bridge slabs under contact explosion. Journal of Constructional Steel Research, 2024; 212: 108223. doi:10.1016/j.jcsr.2023.108223.

[11] Rao, N. N. Static and Dynamic Analysis of Fiber Metal Laminates-A Review. Journal of Failure Analysis and Prevention, 2025; 25: 1576–1591. doi:10.1007/s11668-025-02258-9.

[12] Costa, R. D. F. S., Sales-Contini, R. C. M., Silva, F. J. G., Sebbe, N., Jesus, A. M. P. A Critical Review on Fiber Metal Laminates (FML): From Manufacturing to Sustainable Processing. Metals, 2023; 13: 638. doi:10.3390/met13040638.

[13] Zhuang, Z. Extended Finite Element Formulation. 1st ed. Hoboken (NJ): John Wiley & Sons, Inc.; 2014. doi:10.1002/9781118869673.ch2.

[14] Almustafa, M. K., Nehdi, M. L. Trajectory solution to the reflected blast wave problem. Physics of Fluids, 2025; 37: 116119. doi:10.1063/5.0295470.

[15] Needham, C. E. Blast Waves (Shock Wave and High Pressure Phenomena). 1st ed. Berlin (DE): Springer 2010. doi:10.1007/978-3-642-05288-0.

[16] Le Minh, H., Khatir, S., Abdel Wahab, M., Cuong-Le, T. A concrete damage plasticity model for predicting the effects of compressive high-strength concrete under static and dynamic loads. Journal of Building Engineering, 2021; 44: 103239. doi:10.1016/j.jobe.2021.103239.

[17] SIMULIA Abaqus/CAE User's Manual. 1st ed. Providence (RI): 2012.

[18] Tajmir-Riahi, A., Moshiri, N., Mostofinejad, D. Inquiry into bond behavior of CFRP sheets to concrete exposed to elevated temperatures – Experimental & analytical evaluation. Composites Part B: Engineering, 2019; 173: 106897. doi:10.1016/j.compositesb.2019.05.108.

[19] Xu, Q., Chen, L., Han, C., Harries, K. A., Xu, Z. Experimental research on fire-damaged RC continuous T-beams subsequently strengthened with CFRP sheets. Engineering Structures, 2019; 183: 135–149. doi:10.1016/j.engstruct.2019.01.025.

[20] Li, B., Pan, T.-C., Nair, A. A case study of the structural responses of a tall building in Singapore subjected to close-in detonations. The Structural Design of Tall and Special Buildings, 2011; 20: 223–246. doi:10.1002/tal.531.

[21] Abbas, A., Ahmad, M., Khan, A. H., Alam, J., Ghani, A. Numerical Study on the Behavior of Reinforced Concrete Sandwich Panels (RCSPs) under Blast Load. Iranian Journal of Science and Technology, Transactions of Civil Engineering, 2024; 48: 3049–3068. doi:10.1007/s40996-024-01446-1.

[22] Khalifa, Y. A., Lotfy, M. N., Fathallah, E. Effectiveness of Sacrificial Shielding for Blast Mitigation of Steel Floating Pontoons. Journal of Marine Science and Engineering, 2023; 11: 96. doi:10.3390/jmse11010096.

[23] Building and Housing Research Center (BHRC). Iranian National Building Code, Part 21. Tehran (IR): BHRC; 2016.

[24] Moghimi, H., Driver, R. G. Performance assessment of steel plate shear walls under accidental blast loads. Journal of Constructional Steel Research, 2015; 106: 44–56. doi:10.1016/j.jcsr.2014.11.010.

[25] Abd-El-Nabi, E., El-Helloty, A., Summra, A. Numerical analysis of reinforced concrete buildings subjected to blast load. Structural Concrete, 2023; 24: 3727–3743. doi:10.1002/suco.202200726.

[26] Hussein, A., Heyliger, P. On the accuracy of CEL blast simulations: validation and application. Asian Journal of Civil Engineering, 2025; 26: 843–866. doi:10.1007/s42107-024-01226-2.

[27] Chen, S., Li, Z., Zhang, C., Wen, B., Tang, D. Large deflection analysis of the fully clamped square plates under explosive loading. International Journal of Impact Engineering, 2026; 207: 105514. doi:10.1016/j.ijimpeng.2025.105514.

[28] Syed, Z. I., Raman, S. N., Ngo, T., Mendis, P., Pham, T. The Failure Behaviour of Reinforced Concrete Panels Under Far-field and Near-field Blast Effects. Structures, 2018; 14: 220–229. doi:10.1016/j.istruc.2018.03.009.

[29] Shabanlou, M., Moghaddam, H., Saedi Daryan, A. The Effect of Geometry on Structural Behavior of Buildings with Steel Plate Shear Wall System Subjected to Blast Loading. International Journal of Steel Structures, 2021; 21: 650–665. doi:10.1007/s13296-021-00463-4.

[30] Ngo, T., Mendis, P., Gupta, A., Ramsay, J. Blast Loading and Blast Effects on Structures - An Overview. Electronic Journal of Structural Engineering, 2007; doi:10.56748›ejse.671.

[31] McDonald, B., Bornstein, H., Langdon, G. S., Curry, R., Daliri, A., Orifici, A. C. Experimental response of high strength steels to localised blast loading. International Journal of Impact Engineering, 2018; 115: 106–119. doi:10.1016/j.ijimpeng.2018.01.012.

[32] Norris, G. H., Hansen, R. J., Holly, M. J., Biggs, J. M., S., J. K., Minami Structural Design for Dynamic Loads. 1st ed. Ann Arbor (MI): McGraw-Hill; 1959.

[33] Perry, J. I., Walley, S. M. Measuring the Effect of Strain Rate on Deformation and Damage in Fibre-Reinforced Composites: A Review. Journal of Dynamic Behavior of Materials, 2022; 8: 178–213. doi:10.1007/s40870-022-00331-0.

[34] Liu, Q., Guo, B., Chen, P., Zhai, H., Guo, Y., Tang, S. Experimental investigation blast resistance of CFRP/polyurea composite plates under blast loading. Thin-Walled Structures, 2022; 181: 110149. doi:10.1016/j.tws.2022.110149.

[35] Xu, S., Zhou, S., Zhao, C., Huang, H., Kuang, N., Chen, J., Chen, X., Zhang, W. Strain Rate Effects on the Compressive Behavior of Unidirectional CFRP. Polymer Composites, 2026; 47: 5013–5030. doi:10.1002/pc.70469.